PNL-3385
UC-66

MONITORING INSTRUMENT FIELD EXPERIMENTS AT OREGON INSTITUTE OF TECHNOLOGY

M. J. Danielson
R. P. Smith

MASTER

September 1980

Prepared for
the U.S. Department of Energy
under Contract DE-AC06-76RLO 1830

DISCLAIMER

This book was prepared as an account of work sponsored by an agency of the United States Government. Neither the United States Government nor any agency thereof, nor any of their employees, makes any warranty, express or implied, or assumes any legal liability or responsibility for the accuracy, completeness, or usefulness of any information, apparatus, product, or process disclosed, or represents that its use would not infringe privately owned rights. Reference herein to any specific commercial product, process, or service by trade name, trademark, manufacturer, or otherwise, does not necessarily constitute or imply its endorsement, recommendation, or favoring by the United States Government or any agency thereof. The views and opinions of authors expressed herein do not necessarily state or reflect those of the United States Government or any agency thereof.

Pacific Northwest Laboratory
Richland, Washington 99352

DISTRIBUTION OF THIS DOCUMENT IS UNLIMITED

DISCLAIMER

This report was prepared as an account of work sponsored by an agency of the United States Government. Neither the United States Government nor any agency Thereof, nor any of their employees, makes any warranty, express or implied, or assumes any legal liability or responsibility for the accuracy, completeness, or usefulness of any information, apparatus, product, or process disclosed, or represents that its use would not infringe privately owned rights. Reference herein to any specific commercial product, process, or service by trade name, trademark, manufacturer, or otherwise does not necessarily constitute or imply its endorsement, recommendation, or favoring by the United States Government or any agency thereof. The views and opinions of authors expressed herein do not necessarily state or reflect those of the United States Government or any agency thereof.

DISCLAIMER

Portions of this document may be illegible in electronic image products. Images are produced from the best available original document.

ACKNOWLEDGMENTS

The authors would like to acknowledge Peter Sukvau (Tests 1 and 2) and Dale Lang (Test 3) for collecting the daily field data.

SUMMARY

During 1979 Pacific Northwest Laboratory (PNL) conducted a series of tests in cooperation with Radian Corporation[a] and the Oregon Institute of Technology (OIT) in Klamath Falls, Oregon. The objectives of these experiments were to

- conduct a field evaluation of the instrument probes under development by PNL
- aid OIT in understanding geothermal fluid characteristics that affect the performance of the OIT geothermal space heating system
- assist Radian and OIT in conducting a concurrent materials study.

The field tests were conducted under reducing and oxidizing conditions. Corrosion rates with zero oxygen were about 1.1 mils per year (mpy) for both copper and steel coupons, which is quite low for carbon steel. There was a problem controlling the oxygen level in the oxygenated experiments; however, it was found that corrosion rates increased with the presence of oxygen. Corrosion rates for the steel and copper coupons were 4 and 2 mpy, respectively; copper coupled to cast iron corroded at 8 mpy. Commercial corrosion rate measuring equipment determined the general corrosion rate of carbon steel fairly well but overestimated copper corrosion rates. The redox electrode was a very sensitive indicator of the entry of oxygen.

(a) Radian Corporation, Austin, Texas.

CONTENTS

FIGURES

TABLES

INTRODUCTION

The buildings at the Oregon Institute of Technology (OIT) are heated by geothermal hot water through heat exchanger systems in each building. The main distribution lines are carbon steel; the heat exchangers are constructed of copper and cast iron; and brass valves are used in many locations. Occasional component failures have occurred; however, the causes have not been firmly established. A question has been raised about the suitability of copper and brass for this application since ammonia and H_2S are present in the water. Additional information was needed about those chemical components in the water that may adversely affect system life.

The OIT system is one of the most important nonelectric geothermal heating installations in use today. It is important to the national geothermal effort that the causes of technical problems be established and solutions be found so that satisfactory recommendations can be made to others who may be considering geothermal heating.

In response to this concern Pacific Northwest Labortory (PNL),[a] Radian Corporation,[b] and OIT conducted a series of tests to

- evaluate the in-field performance of instrument probes being developed by PNL
- aid OIT in understanding geothermal fluid characteristics as they affect the geothermal heating system
- assist Radian and OIT in a concurrent materials study.

This cooperative series of tests required the development of a portable in-line package to characterize geothermal fluids and measure their effects on materials using advanced electrical probe methods and standard coupon tests. Provisions were included in the package so that OIT and Radian could conduct a simultaneous materials study.

(a) Operated for the U.S. Department of Energy (DOE) by Battelle Memorial Institute.
(b) Radian Corporation, Austin, Texas, (hereafter referred to as Radian) is under contract to DOE, Geothermal Energy Division, to evaluate materials in the geothermal environment.

CONCLUSIONS AND RECOMMENDATIONS

From the test it was found that entry of oxygen into the geothermal system increases corrosion rates. In particular, the crevice corrosion rate of steel increased from 13 to 50 mils per year (mpy), and the general corrosion rate of copper coupled to cast iron (graphite-exposed) increased from 2.5 to 7.8 mpy with low levels of oxygen. This condition--copper coupled to cast iron--was investigated because copper heat exchanger tubing penetrates a cast iron tube plate and carbon/graphite contamination may occur at copper-sweated joints. In general, oxygen intrusions must be prevented for maximum system life. This is particularly important in thin-walled copper tubing.

Commercial corrosion rate measuring instruments (Petrolite)[a] determined the corrosion rate of carbon steel within a factor of two (compared to weight loss determinations) but considerably overestimated the corrosion rate of copper. Fortunately, the instruments do respond to the entry of oxygen by indicating increased corrosion rates.

The redox electrode was a very sensitive indicator of oxygen entry and could be used as an oxygen monitor to help maintain low oxygen levels.

(a) Petrolite, Houston, Texas.

FIELD TEST CONDITIONS

Three tests were planned for the evaluation. PNL set up the experiments, and an OIT student carried out the daily measurements. Test 1 included a redox probe (oxidation-reduction potential), a pH probe, a PNL-developed corrosion probe, and a commercial corrosion probe (Petrolite). It was conducted with deoxygenated geothermal water flowing directly from the well at the highest flow rate (initially 5 ft/sec in the specimen holder test section).

Test 2 was also conducted in deoxygenated water but at a lower flow rate (0.5 ft/sec) to determine the effects of velocity. Test 3 was performed in oxygenated brine at the high flow rate of 5 ft/sec; this test was considered the worst case for corrosive effects.

The responsibilities of the participants--PNL, Radian, and OIT--during the evaluation were to

- design the portable in-line package and develop the test plan (PNL)
- fabricate and test the loop, evaluate in-line probes, and monitor water chemistry (PNL)
- determine corrosion rates on weight loss, stress, and crevice specimens (Radian)
- analyze the specimens after the tests to determine the extent of the corrosion (Radian)
- provide the geothermal fluid access (OIT)
- provide an operator to monitor the tests on a daily basis (OIT).

Figure 1 is a schematic of the test loop, Figure 2 details the specimen holder, and Figure 3 is a photograph of the test loop. The original experimental approach is summarized in Table 1.

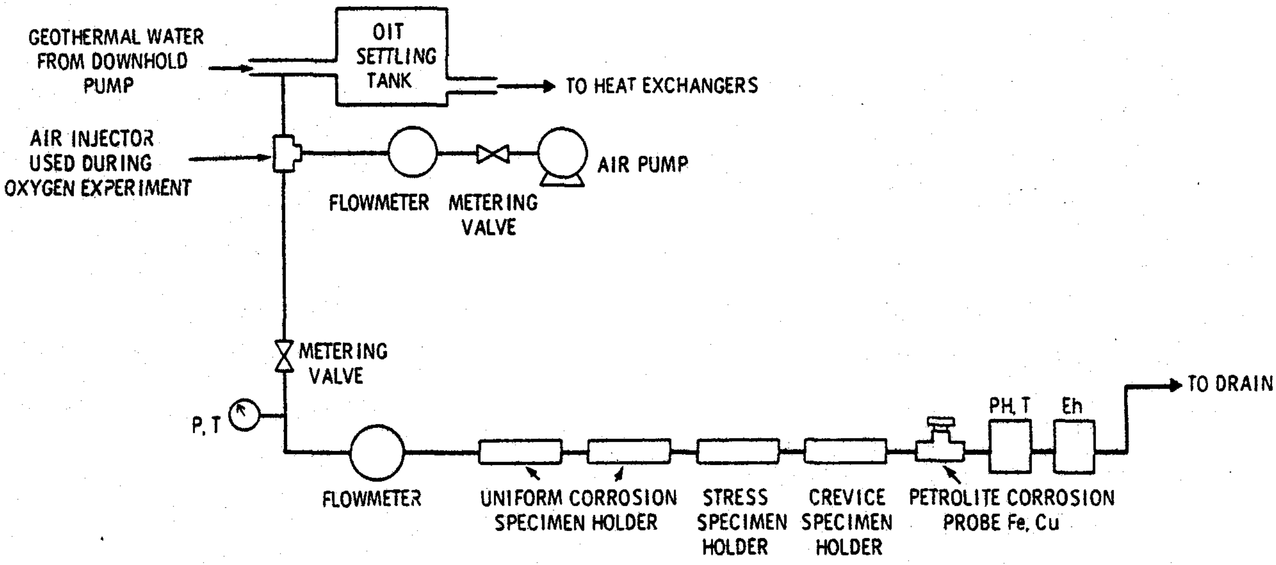

FIGURE 1. Schematic of Test Loop (not to scale, built of 1/2-in. pipe)

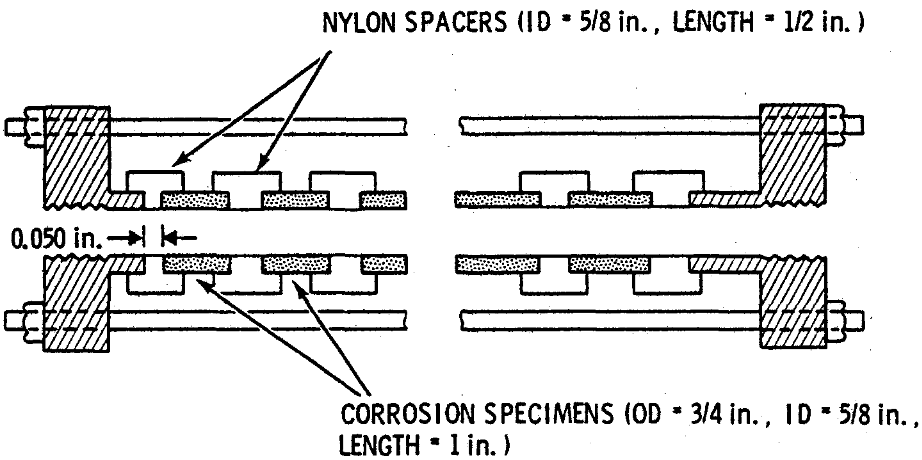

FIGURE 2. Cross Section of Specimen Holder

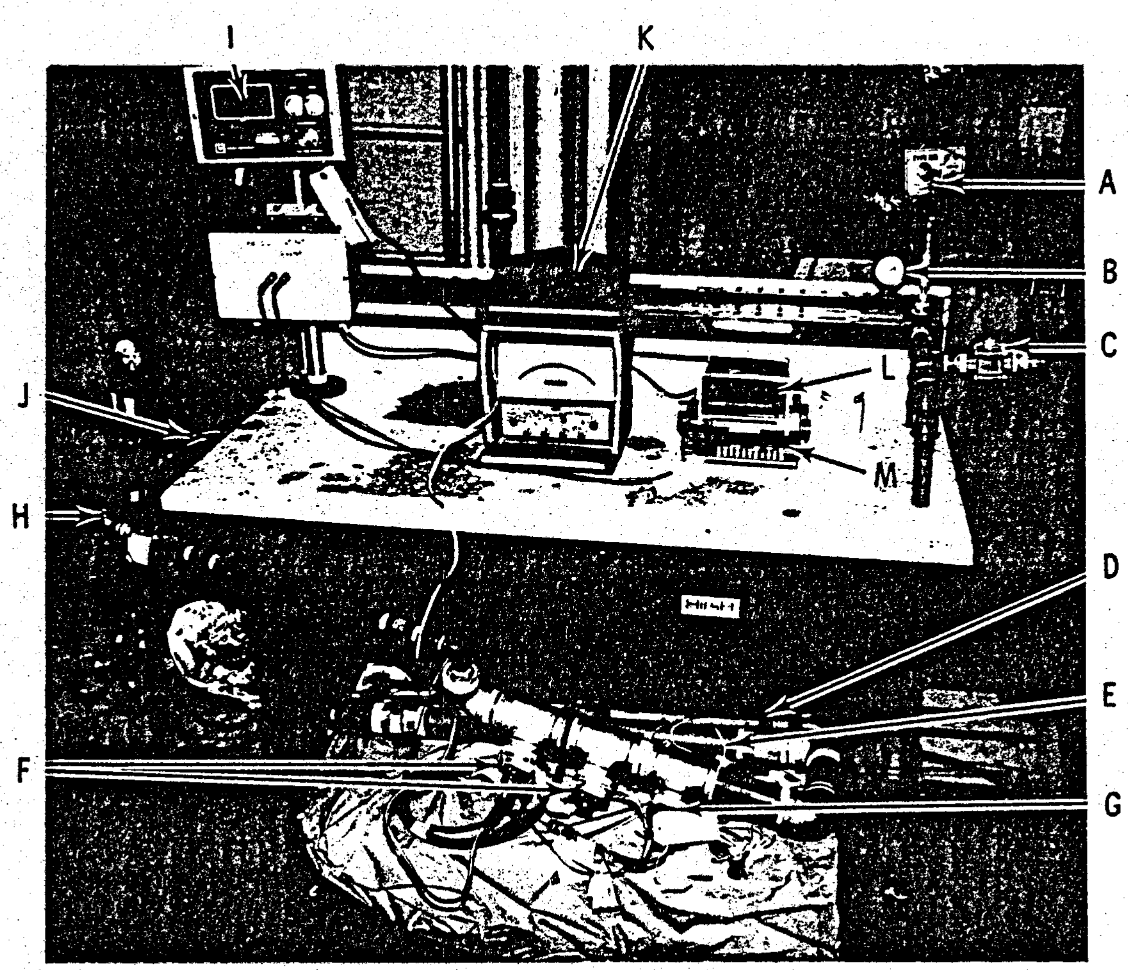

A INLET TEMPERATURE

B INLET PRESSURE

C INLET SAMPLING VALVE

D WEIGHT LOSS COUPON LEG

E STRESS AND CREVICE COUPON LEG

F Fe AND Cu PETROLITE PROBES

G REDOX PROBE

H INLINE pH PROBE, OUTLET TEMPERATURE

I pH READOUT

J FLEXIBLE HOSE TO DRAIN

K CORROSION READOUT

L TEMPERATURE READOUT

M REDOX READOUT

0 6 12

INCHES

FIGURE 3. Portable In-Line Package at Test Site at OIT

TABLE 1. Summary of Experimental Approach

PNL	Radian
• Set up three tests: 1) Deoxygenated brine at 5 ft/sec 2) Deoxygenated brine at 0.5 ft/sec 3) Oxygenated brine at 5 ft/sec Each test scheduled for 3-6 weeks depending on corrosion rates	• Weight loss corrosion specimens to be pipe sections 1 in. long with inside diameter (ID) = 5/8 in. Materials will be DHP copper, A53B carbon steel, 316 stainless steel (SS), titanium (grade 2), DHP copper in contact with graphitized cast iron, and Admiralty brass (type 443 used in valves). Three samples of each will be included.
• Volumetric flow rate for test sections at 5 ft/sec is 4.7 gal/min	• Specimens of 316 SS, DHP copper, and Admiralty brass will be stressed at 100% of yield strength in a C-ring arrangement for stress cracking studies. There will be three specimens of each material.
• Chemistry to be monitored with pH and Eh (redox) probes and by sampling and lab analysis	
• Instantaneous corrosion rates to be followed using polarization resistance technique on separate specimens (not involved in weight loss tests) of deoxidized (DHP) copper and A53B carbon steel. Weight loss specimens to be included in each test for comparison; three specimens of each material will be required. Commercial electrode units (Fe and Cu) to be installed.	• Specimens of DHP copper, 316 SS, and A53B carbon steel will be used in a crevice corrosion experiment. Three specimens of each material will be provided.

PNL PROBE STUDIES

In-line probes offer unique advantages since continuous output is available and, in general, less time is required to make measurements. Continuous output also offers the advantage of detecting transient conditions that would go unobserved by conventional methods.

The instrument probes that were field-tested included an in-line redox probe (oxidation-reduction potential), pH probe, and corrosion probes (which measure the instantaneous corrosion rate by the polarization resistance method). A commercially available corrosion instrument (Petrolite) was combined with PNL electrodes as well as with Petrolite corrosion electrodes for comparison. The corrosion probe systems are compared in Figure 4.

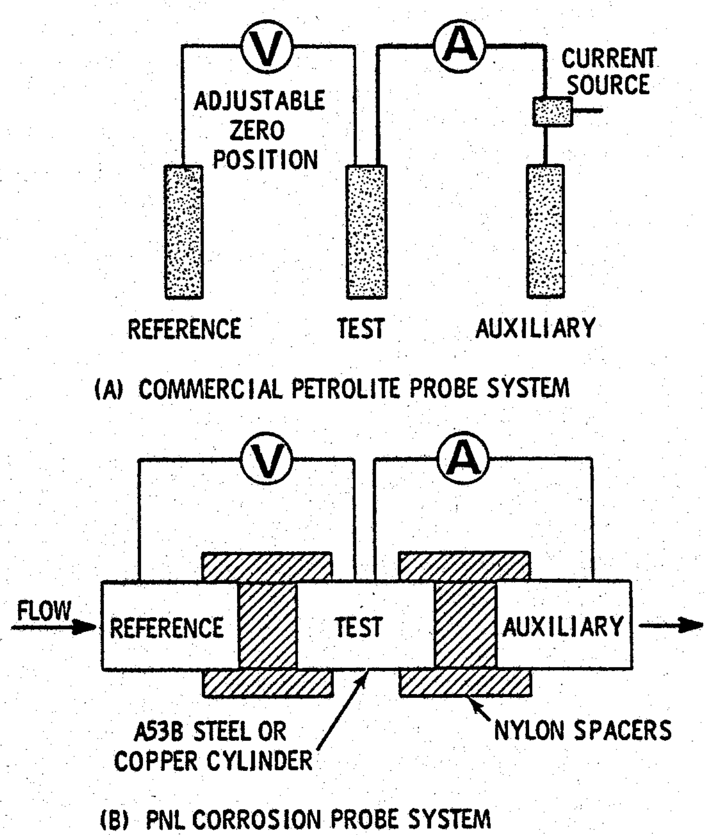

FIGURE 4. Comparison of Petrolite and PNL Corrosion Probes

To measure corrosion rates, the potential of the test electrode is perturbed by +10 and -10 mV from the freely corroding potential, and the current is measured at each potential. This current is directly proportional to the corrosion rates (Fontana and Staehle 1976). For greater accuracy, the corrosion rate at +10 mV was averaged with the corrosion rate at -10 mV. The PNL corrosion probe system uses cylindrical specimens in the specimen holder (see Figure 2), which subjects the specimens to the same flow conditions as the weight loss coupons. The corrosion probe specimens are not used for weight loss determinations. Petrolite probe sets of copper (99.9%) and 1018 steel were also tested.

Tubing sections of titanium, 316 SS, Admiralty brass, A53B carbon steel, and copper (see Table 2 for specifications) were mounted in the specimen holder

TABLE 2. Alloy Compositions

Material	Composition, %	Material	Composition, %
316 SS	0.08 C[a]	Admiralty Brass	1 Sn
	0.75 Si[a]	(LA 443)	28 Zn
	0.04 P[a]		71 Cu
	11-14 Ni		
	16-18 Cr	Titanium	0.1 C[a]
	Remainder Fe	(Grade 2)	0.20 Fe[a]
			0.25 O[a]
A53B	0.23 C		Remainder Ti
Carbon Steel	0.71 Mn		
	0.15 Si	1018 Steel	0.15-0.20 C
	0.01 P	(Petrolite	0.60-0.90 Mn
	0.26 Ni	Electrodes)	0.040 P[a]
	Remainder Fe		0.050 S[a]
			Remainder Fe
DHP Copper	0.015-0.040 P		
	99.9 Cu		

(a) maximum

(Figure 2) with nylon spacers providing electrical insulation and the pressure seal. With this arrangement liquid velocity, which is an important corrosion parameter, can be controlled. Three specimens of each metal were used for weight loss measurements, and three specimens of both copper and A53B carbon steel were used as corrosion probes for measurements with the PNL probe system. Weight loss was measured for one copper specimen that was electrically connected (externally) to a cast-iron specimen to simulate a special corrosion condition found in the OIT system.

The crevice- and C-ring-stressed specimens were placed in a PVC tube as seen in Figure 3 (Item E). Artificial crevices (~0.005 in. deep) were made using insulated titanium bolts to hold identical pieces of tubing together. The C-rings were stressed to 100% yield strength with insulated titanium bolts using the recommmended ASTM method (ASTM Standard 1978).[a]

Figure 3 also shows two Petrolite corrosion probes mounted so that gas bubbles will not be trapped. The entire loop was mounted so that the outlet from each portion was higher than the inlet of the next portion to prevent gas accumulation.

The pH system, mounted at the end of the loop, was a Leeds and Northrup unit (North Wales, Pennsylvania) consisting of a transmitter, receiver, ryton cell (model 7777), combination pH-reference electrode (#117486), and temperature compensator. For standardization, the plastic boot on the bottom of the electrode was removed, buffer was poured in, the boot was replaced, and brine was passed through the loop. When the pH electrode had reached operating temperature, the pH meter was standardized. At that point in the experiment the brine was shut off, the boot was removed, the pH electrode was inserted into the brine, and the brine flow was restarted. The pH electrode was operating at close to the maximum limits recommended by the manufacturer. Standardization was checked several times during each experiment and very little drift was found.

The redox electrode consisted of a platinized platinum electrode and a PNL-developed reference electrode (Danielson 1979). The reference electrode

(a) 1978 Annual Book of ASTM Standards Designation G38-73.

permits the potential to be placed on the hydrogen scale. Potential difference was measured using a high-input impedance voltmeter.

A local OIT operator monitored and recorded daily measurements from corrosion probes; redox, pH, and temperature meters; and flow and pressure gauges. Table 3 is a log of the daily measurements taken during Test 1, and Table 4 provides similar data for Test 3.

TABLE 3. Daily Measurements Taken During Test 1 at OIT

Data \ Date			4-17-79 18:00	4-17-79 22:00	4-18-79 9:00	4-18-79 11:30	4-18-79 15:00	4-19-79 10:15	4-19-79 17:00	4-20-79 15:15	4-21-79 8:30	4-22-79 13:30	4-23-79 16:15	4-24-79 17:15	4-25-79 16:00	4-26-79 17:45	4-27-79 17:15	4-28-79 18:45	4-29-79 16:15	4-30-79 20:30
Inlet Temperature (T-1)		°C	89	89	89	89	89	89	89	89	89	89	89	89	89	89	89	89	89	89
Inlet Pressure (P-1)		psig	5.8	5.3	5.1	6.0	6.0	6.5	6.0	6.4	6.0	6.0	6.5	5.7	6.3	6.0	6.2	6.3	6.2	5.8
Petrolite Fe-2	anodic	MPY	20	6.0	3.2	3.5	1.8	2.0	1.2	2.4	2.2	2.1	2.0	1.6	2.0	2.1	2.1	1.4	2.4	2.6
	cathodic	MPY	20	6.5	3.9	3.3	3.1	3.0	1.5	3.3	2.8	2.7	2.7	2.9	2.8	2.6	2.4	2.8	2.4	2.4
Petrolite Cu-2	anodic	MPY	12	4.5	5.2	4.5	5.0	4.9	2.5	3.6	2.9	3.0	2.3	2.4	3.0	3.3	3.6	3.5	4.2	4.4
	cathodic	MPY	14	3.3	2.6	3.0	2.5	2.5	2.3	2.7	2.4	2.9	3.3	3.3	3.2	2.7	2.6	2.8	2.8	2.6
Probe Fe-1	anodic	MPY	20	20	15	11.0	8.6	4.5	1.1	1.4	0.8	0.9	1.0	0.8	0.9	0.7	0.4	1.0	0.6	0.5
	cathodic	MPY	15.5	14.4	11	9.0	6.4	4.1	0.9	0.7	0.7	0.9	0.6	0.6	0.7	0.7	0.8	0.8	0.8	0.6
Probe Cu-1	anodic	MPY	13.5	5.0	2.5	3.1	3.5	8.1	6.4	4.0	4.2	4.4	3.8	3.2	3.0	3.2	2.9	3.1	3.0	3.2
	cathodic	MPY	7	2.0	1.6	1.5	1.4	1.9	2.7	1.6	1.5	1.4	1.6	1.6	1.6	1.7	1.7	1.6	1.7	1.8
Flow Rate		GPM	4.75	4.55	4.70	4.75	4.70	4.8	4.6	4.75	4.7	4.55	4.80	4.55	4.7	4.7	4.7	4.7	4.8	4.65
Eh		Volts	-0.586	-0.629	-0.602	-0.609	-.566	-0.568	-0.511	-0.545	-0.560	-0.564	-0.558	-0.553	-0.561	-0.560	-0.565	-0.564	-0.566	-0.555
pH		-----	8.06	8.03	8.00	7.91	7.89	7.90	7.90	7.81	7.86	7.82	7.82	7.80	7.79	7.80	7.77	7.79	7.78	7.76
Outlet Temperature (T-2)		°C	88	88	88	88	88	88	88	88	88	88	88	88	88	88	88	88	88	88

Data \ Date			5-1-79 22:00	5-2-79 23:00	5-3-79	5-4-79	5-5-79	5-6-79 22:00	5-7-79 21:15	5-8-79 15:00	5-9-79 14:00	5-10-79 14:30	5-11-79 15:00	5-12-79 14:30	5-13-79 20:15	5-14-79 22:15	5-15-79 20:15	5-16-79 22:15	5-17-79 22:00	5-18-79 22:00	5-19-79 18:30	5-20-79 18:30	5-21-79 9:45
Inlet Temperature (T-1)		°C	87	87				88	88	88	88	88	88	88	88	88	87	87	87	87	87	87	87
Inlet Pressure (P-1)		psig	6.0	5.8				5.0	6.0	5.8	6.0	6.2	6.0	6.2	6.0	6.0	6.2	5.2	5.8	5.8	6.0	4.5	3.0
Petrolite Fe-2	anodic	MPY	0.1	0.4				2.0	1.2	1.4	1.2	1.1	0.7	0.5	2.0	1.9	0.8	0.8	1.0	0.6	0.3		1.5
	cathodic	MPY	1.9	1.6				2.4	2.7	2.8	1.7	1.2	1.3	2.0	2.5	2.7	1.2	1.4	2.4	1.6	1.8		2.6
Petrolite Cu-2	anodic	MPY	6.9	5.8				4.1	4.0	4.4	4.3	6.4	5.1	5.9	6.3	6.0	4.7	4.6	6.3	7.2	6.5		7.2
	cathodic	MPY	4.2	3.2				3.1	2.0	2.1	2.4	3.1	2.5	2.4	2.2	2.4	2.8	2.5	2.0	2.4	2.8		4.5
Probe Fe-1	anodic	MPY	0.8	0.5				0.7	0.5	0.6	0.6	1.6	1.8	2.2	1.7	1.8	0.8	0.9	0.8	0.7	1.2		1.3
	cathodic	MPY	0.9	1.0				0.6	0.4	0.5	0.6	2.6	2.4	2.4	2.4	2.3	0.8	0.8	0.4	0.9	2.0		2.2
Probe Cu-1	anodic	MPY	9.9	6.4				4.7	3.2	4.2	4.5	3.8	4.4	4.2	4.5	4.4	4.5	4.3	4.6	6.9	6.9		7.4
	cathodic	MPY	5.6	5.6				2.7	2.0	2.2	2.2	2.4	2.4	2.6	2.4	2.6	2.3	2.6	2.2	2.4	2.1		1.7
Flow Rate		GPM	4.7	4.7				4.7	4.7	4.7	4.7	4.7	4.65	4.7	4.65	4.7	4.7	4.7	4.7	4.7	4.7	4.75	3.6
Eh		Volts	-0.458	-0.47				-0.530	-0.540	-0.562	-0.540	-0.584	-0.584	-0.608	-0.623	-0.633	-0.591	-0.598	-0.590	-0.563	-0.600	-0.414	-0.559
pH		-----	7.78	7.77				7.72	7.69	7.70	7.69	7.66	7.68	7.67	7.64	7.65	7.66	7.72	7.67	7.66	7.63	7.76	7.65
Outlet Temperature (T-2)		°C	86	86				87	87	87	87	87	87	87	87	87	86	85	86	86	86		86

TABLE 4. Daily Measurements Taken During Test 3 at OIT

Data / Date			9-6-79 14:35	9-10-79 15:25	9-11-79 14:30	9-13-79 16:20	9-14-79 15:55	9-15-79 17:30	9-16-79 17:25	9-17-79 14:55	9-18-79 14:20	9-19-79 19:55	9-20-79 19:45	9-21-79 15:50	9-22-79 19:00	9-23-79 18:30	9-24-79 16:15	9-25-79 15:38	9-26-79 16:20	9-27-79 13:30
Inlet Temperature	(T-1)	°C	87	87	87	87	87	86	86	87	87	88	88	88	87	88	88	88	88	88
Inlet Pressure	(P-1)	psig	1.3	1.3	1.3	0.5	0.02	0	0	1.2	1.3	1.4	1.3	1.5	1.5	1.5	1.5	1.5	1.5	1.5
Petrolite Fe-2	anodic	MPY	2.8	1.4	2.2	3.2	1.8	1.0	2.0	2.0	2.7	1.4	3.8	2.0	2.0	2.5	2.5	3.0	3.0	2.6
	cathodic	MPY	6.2	5.8	5.6	4.8	4.8	5.8	4.4	6.0	5.1	6.4	5.4	5.5	6.0	6.2	5.8	5.2	5.4	5.4
Petrolite Cu-2	anodic	MPY	3.5	5.4	5.0	5.4	4.8	5.2	5.5	6.3	5.3	5.5	6.4	5.3	5.8	5.5	5.2	6.2	6.4	6.1
	cathodic	MPY	4.5	6.4	6.4	2.45	8.0	7.8	7.4	7.8	8.5	7.4	7.2	8.2	7.5	7.8	8.8	8.5	8.2	8.2
Probe Fe-1	anodic	MPY	47	12.0	12.0	10.4	7.5	8.2	10.4	10.2	9.2	10.3	12.4	16.2	11.0	12.0	11.6	12.4	12.2	10.4
	cathodic	MPY	14	3.5	3.0	4.4	6.2	5.4	3.6	4.8	5.4	3.8	4.8	3.0	6.0	4.4	6.8	5.8	6.0	6.0
Probe Cu-1	anodic	MPY	2.0	7.2	7.2	6.4	6.4	3.5	6.4	5.3	5.8	3.0	5.2	2.0	4.0	2.4	6.0	4.5	4.0	10.0
	cathodic	MPY	5.0	7.8	6 0	3.2	5.8	5.8	5.3	6.4	5.0	4.0	6.8	5.8	6.4	6.4	5.7	6.5	5.8	6.2
Flow Rate		GPM	2.7	2.74	2.74	2.45	3.75	4.55	4.55	---	---	---	---	---	---	---	---	---	---	---
Eh		volts	+.320	+.446	+.464	+.469	+.464	+.481	+.490	+.52	+.539	+.543	+.551	+.551	+.540	+.551	+.550	+.551	+.551	+.558
pH		---	7.73	7.76	7.74	7.74	7.75	7.76	7.75	7.73	7.72	7.72	7.72	7.71	7.72	7.71	7.71	7.70	7.70	7.70

GEOTHERMAL WATER CHEMISTRY RESULTS

The geothermal water chemistry was determined (Watson 1978) at OIT wellheads 2, 5, and 6, which were used in various combinations to feed the test loop (see Table 5). The water chemistries of these three wells were remarkably similar; and as far as corrosion and probe tests are concerned, a constant water chemistry was supplied. One side effect, a short-term introduction of oxygen into the system due to exchanging the feeder well(s), provided an interesting test for the probes. The responses of the probes to this perturbation will be discussed later in this report.

The water chemistry and temperature similarities of these three wells implies that they are feeding from the same reservoir. Using an average SiO_2 concentration of 100 mg/l the quartz geothermometer of Fournier and Truesdell (1974) predicts a down-hole temperature of 137°C. The observed temperature of 89°C suggests that the geothermal water is diluted by a cooler reservoir or cooled on its trip up the well. Another interesting characteristic of OIT geothermal water is that it is a sulfate-buffered system as compared to the more common carbonate-buffered geothermal water systems.

In comparing chemical data between the inlet and outlet of the test loop (Table 5), it is clear that during Test 1 the water chemistry remained constant. Thus, any chemical changes in water properties due to corrosion are not large enough to be noticed in this short test loop. It is important to note that the dissolved oxygen value was not greater at the outlet, which verifies that there were no leaks during Test 1. Temperature, pressure, flow rate, pH, and Eh of the geothermal water were measured daily (see Table 3 for Test 1 and Table 4 for Test 3). There was a slow minor decline in the pH value; the source of which is not known. Nevertheless, these tables show that major perturbations in pH and water chemistry did not occur during the tests.

The water chemistry was also analyzed during Test 1 at several other locations (Table 5) in the OIT geothermal heating system. These tests verified that the water chemistry used to obtain corrosion data in the test loop was similar in composition to the water in the OIT heating system. It is

TABLE 5. Water Chemistry Data Plus Method of Determination at Various Locations at OIT. Concentrations are mg/ℓ or as noted. Al through Zr were determined by Argon Plasma Emission Spectrometer.

PARAMETER \ SAMPLE ID	OIT Well #6 10-30-78	OIT Classroom Bldg. (Owens) 10-30-78	OIT Lab #2 10-30-78	OIT Well #2 4-17-79	OIT Well #6 4-17-79	Test Inlet 4-19-79	Test Outlet 4-19-79	Test Inlet 5-7-79	OIT Well #5 5-7-79
pH	8.68	8.71	8.52	8.65	8.66	8.65	8.65	8.72	8.70
CONDUCTIVITY	1040 µmhos/cm	1020 µmhos/cm	1045 µmhos/cm	840 µmhos/cm	840 µmhos/cm	820 µmhos/cm	810 µmhos/cm	860 µmhos/cm	860 µmhos/cm
TDS	791	794	800	789	798	793	796	780	778
SUSPENDED SOLIDS	ND[1]	ND[1]	ND[1]	ND[1]	ND[1]	ND[1]	ND[1]	ND[1]	ND[1]
TURBIDITY	ND[1]	ND[1]	ND[1]	3 FTU	ND[1]	ND[1]	ND[1]	2 FTU	3 FTU
HCO_3^- (TITRATION)	20	ND[1]	22	30	31	32	42	33	32
$CO_3^=$ (TITRATION)	15	23	14	3.9	ND[1]	5.9	ND[1]	6.3	6.5
$SO_4^=$ (TURBIDIMETRIC)	330	330	325	340	340	360	340	350	370
$SO_4^=$ (ION CHROM.)	372	387	368	378	395	388	386	376	368
F^- (ION CHROM.)	1.5	1.3	1.6	1.2	1.3	1.3	1.4	0.9	0.6
Cl^- (TITRATION)	51	49	48	48	49	49	49	48	47
NH_3 (ELECTRODE)	1.3 (1.1-Nessler.)	0.9 (0.9-Nessler.)	1.1 (0.9-Nessler.)	<0.2	0.2	0.3	0.5	1.4	1.3
SiO_2 (COLORIMETRIC)	95	---	---	79	76	74	76	85	83
NO_3^- (COLORIMETRIC)	4.9	5.0	4.8	<0.25	<0.25	<0.25	<0.25	<0.25	<0.25
OTHER: H_2S ($Zn(OAc)_2$ sample)	1.5	---	---	0.5	0.3	0.3	0.3	0.4	0.3
CO_2 (NaOH sample)	32	---	---	40	37	32	37	60	43
Temp. (field)	90°C	20°C	19°C	84°C	89°C	86 (to samples) 89 (to test fac.)	84°C	87°C	84°C
Pressure (field)	53 psig	---	---	51 psig	52 psig	12 psig	6 psig	7.3 psig	32 psig
Flow (field)	200 GPM (estimate)	---	---	---	---	4.7 GPM	4.7 GPM	4.7 GPM	---
pH (field)	8.4 (@40°C)	8.8 (@20°C)	---	8.7 (25°C)	8.7 (28°C)	8.7 (28°C)	8.7 (12°C)	8.9 (20°C)	8.9 (20°C)
O_2 (field)	0 ppb (near valve) 15 ppb (inlet to filter & heat exch. bldg.)	0 ppb	60 ppb	---	---	0 ppb	0 ppb	5 ppb	0 - 5 ppb
Cl (ION CHROM.)	---	---	---	43	43	46	49	52	63
K (ION CHROM.)	4.3	3.5	4.1	4.2	4.5	4.6	5.1	2.5	2.5
NH_4[3] (field)	---	---	---	0.8	0.6	0.6	0.4 - 0.6	0 - 0.1	0 - 0.1
H_2S (field)	---	---	---	0.1	0.1	0.2	0.2	0.1	0.1
NH_3 (ION CHROM.)	---	---	---	<1.0	<1.0	<1.0	<1.0	---	---
Al	<0.02	<0.02	<0.02	<0.10	<0.10	<0.10	<0.10	0.10	0.10
As	0.05	<0.03	<0.03	<0.05	<0.05	<0.05	<0.05	0.10	<0.05
B	1.01	0.93	0.95	0.90	0.92	0.89	0.89	0.99	0.97
Ba	0.003	0.002	0.002	<0.01	<0.01	<0.01	<0.01	<0.01	<0.01
Ca	26	29	25	23	24	24	24	25	25
Fe	0.01	0.01	0.25	<0.10	<0.10	<0.10	<0.10	<0.10	<0.10
K	---	---	---	---	---	---	---	---	---
Li	0.2	0.2	0.2	0.18	0.18	0.16	0.15	0.16	0.16
Mg	0.02	0.02	0.02	<0.05	<0.05	<0.05	<0.05	<0.05	<0.05
Na	205	197	201	240	250	230	220	240	240
P	<0.09	<0.09	<0.09	<0.05	<0.05	<0.05	<0.05	<0.05	<0.05
Si	48 (103 as SiO_2)	43 (92 as SiO_2)	44 (94 as SiO_2)	39	39	38	38	40	39
Sr	0.3	0.3	0.2	0.27	0.29	0.28	0.28	0.32	0.32
Ag	<0.03	<0.03	<0.03	<0.01	<0.01	<0.01	<0.01	<0.01	<0.01
Cd	<0.01	<0.01	<0.01	<0.01	<0.01	<0.01	<0.01	<0.01	<0.01
Co	<0.01	<0.01	<0.01	<0.01	<0.01	<0.01	<0.01	<0.01	<0.01
Cr	<0.01	<0.01	<0.01	<0.05	<0.05	<0.05	<0.05	<0.05	<0.05
Cu	<0.01	<0.01	<0.01	<0.01	<0.01	<0.01	<0.01	<0.01	<0.01
Mn	<0.01	<0.01	<0.01	<0.01	<0.01	<0.01	<0.01	<0.01	<0.01
Mo	<0.01	<0.01	<0.01	<0.50	<0.50	<0.50	<0.50	<0.50	<0.50
Ni	<0.02	<0.02	<0.02	<0.01	<0.01	0.01	0.01	0.01	0.01
Pb	<0.02	<0.02	<0.02	<0.10	<0.10	<0.10	<0.10	<0.10	<0.10
Sb	<0.03	<0.03	<0.03	<0.05	<0.05	<0.05	<0.05	<0.05	<0.05
Se	<0.02	<0.02	<0.02	<0.10	<0.10	<0.10	<0.10	<0.10	<0.10
Sn	<0.03	<0.03	<0.03	<0.10	<0.10	<0.10	<0.10	<0.10	<0.10
Th	<0.1	<0.1	<0.1	<0.10	<0.10	<0.10	<0.10	<0.10	<0.10
Ti	<0.08	<0.08	<0.08	<0.05	<0.05	<0.05	<0.05	<0.05	<0.05
Tl	<0.08	<0.08	<0.08	<0.10	<0.10	<0.10	<0.10	<0.10	<0.10
U	<0.08	<0.08	<0.08	<0.05	<0.05	<0.05	<0.05	<0.05	<0.05
Zn	<0.02	<0.02	<0.02	<0.05	<0.05	<0.05	<0.05	<0.05	<0.05
Zr	<0.01	<0.01	<0.01	<0.05	<0.05	<0.05	<0.05	<0.05	<0.05

REMARKS:

A. Gas/Liquid Vol. Ratio from OIT Well #6 (10-30-78) - 16 ml gas/(liter brine)

B. Gas Sample at OIT Well #6 (corrected for air contamination)

Mole % (Mass Spec.)

CO_2	Ar	O_2	N_2	CO	He	H_2	CH_4
0.3	1.4	--	94.2	<0.8	<0.1	0.1	4.0

C. Gas/Liquid Weight Ratio (OIT Well #6) - 18 mg/Kg brine)
- Based on mass spec. analysis and weighted average mole weight of gas = 28 g/mole

D. Analysis of liquid from gas/liquid ratio gas sampling bulb run immediately for H_2S by methylene blue colorimetric method gave 0.05 mg H_2S/(liter brine). This was an unstabilized sample.

E. Footnotes

ND[1] - None Detected

H_2S[2] - Chemetrics Kit

NH_4[3] - Chemetrics Kit

important to note that oxygen does enter the system downstream from the OIT storage tank. During Test 1, the OIT storage tank was not vented to the atmosphere and oxygen was excluded; usually the storage tank is vented and oxygen does enter the system at this point.

CORROSION RESULTS

TEST 1

Due to mechanical problems not associated with the test loop, the geothermal water supply was switched several times during Test 1. Geothermal water was initially supplied from OIT wells 2 and 6, then well 5, and finally wells 2 and 5. In some cases, air entered the system during the changeover. Flow rate was held to about 5 ft/sec in the test sections containing pipe samples, and the inlet temperature was 85 to 89^{o}C. The pH (measured and standardized at 86 to 88^{o}C) varied from 8.0 to 7.7. The wells all contained H_2S ranging from 0.3 to 0.5 ppm and NH_3 ranging from 0.2 to 1.3 ppm. Oxygen was measured to be 0 ppb at the inlet and outlet of the test loop at the beginning of the experiment.

The redox electrode responds to the general "oxidativeness" of the environment, and the potential becomes less negative when oxygen enters the system. It is uncertain what electrochemical reactions the platinized platinum electrode is responding to, but it does perform the important function of indicating the presence of oxygen. The redox potential (based on the standard hydrogen potential) as a function of time is shown in Figure 5. The experimental potentials (based on an Ag/AgCl reference electrode) are placed on the standard hydrogen electrode (SHE) scale by adding 0.23 V to the measured potential. The electrode clearly responds to oxidizing and reducing conditions. It should be pointed out that only one data point was taken each day, and the redox potential may not be responding to the peak oxygen concentration at the time of the measurement. A small amount of oxygen was permitted to enter at the start of the experiment, and the redox potential shifted (positive direction) by more than 350 mV, which demonstrates the magnitude of the response.

The combination pH-reference electrode (Leeds and Northrup, North Wales, Pennsylvania) was operating close to the maximum recommended operating temperature. Periodically, the electrode was restandardized with a pH-7 buffer at the process temperature to determine how well the calibration was holding. Typically, the calibrated pH would shift by less than 0.1-pH unit, which

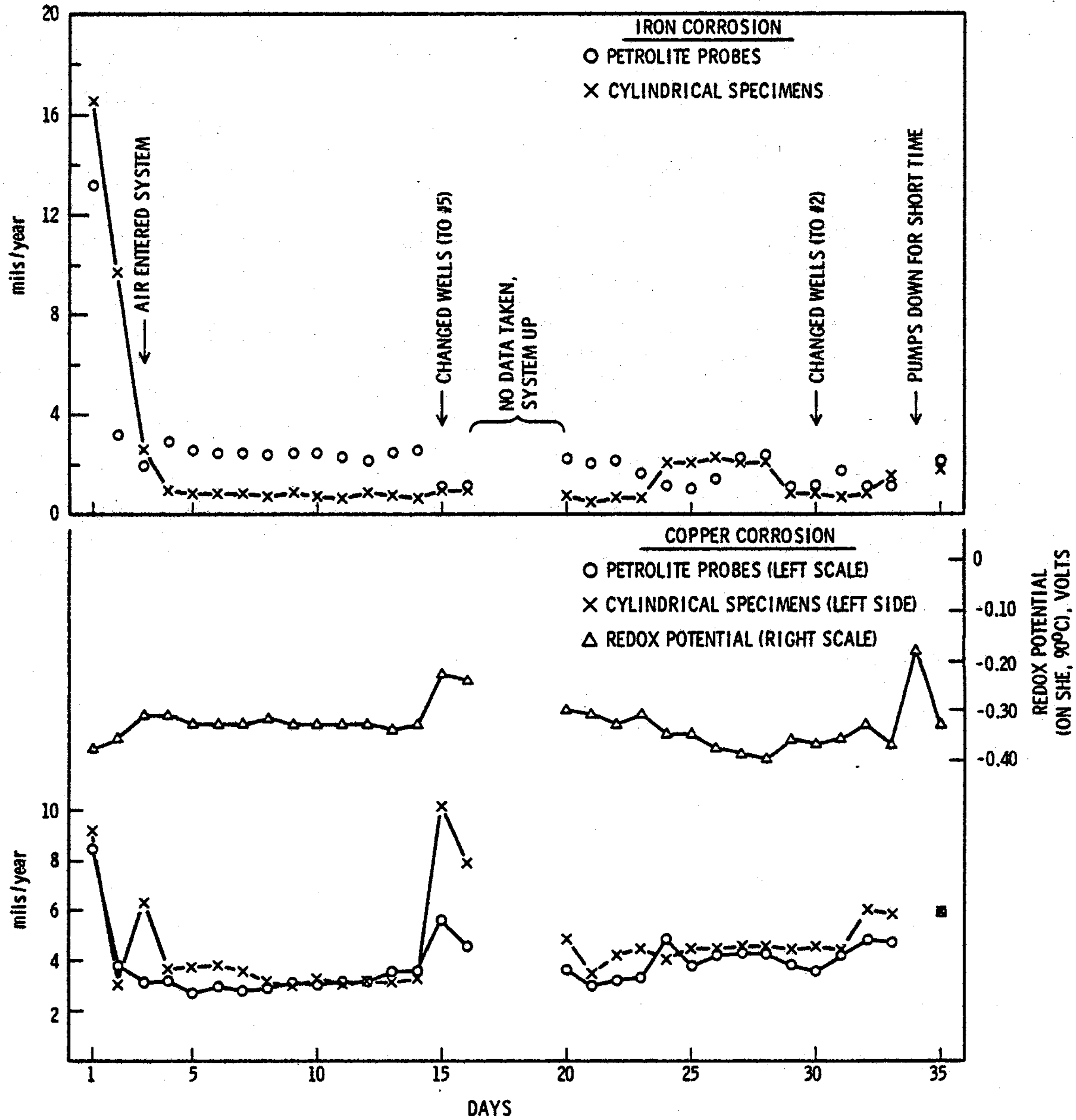

FIGURE 5. Corrosion Rates of Petrolite and PNL Probes Versus Days of Exposure, Test 1

indicates fairly good reliability. Nernstian response was checked by using different pH buffers at the start of the experiment.

Radian's evaluation (Ellis 1980) of the corrosion coupons is reported in Tables 6 and 7. In summary,

- Carbon steel had a uniform corrosion rate of 1.1 mpy and a crevice corrosion rate of 13 mpy.
- Copper had a uniform corrosion rate of 1.1 mpy with incipient crevice corrosion but no evidence of stress corrosion cracking (SCC).
- Brass corroded at 0.4 mpy with incipient crevice corrosion but no evidence of SCC.
- 316 SS corroded uniformly at 0.1 mpy with no evidence of crevice corrosion or SCC.
- Titanium had a negligible uniform corrosion rate with no evidence of crevice corrosion or SCC.
- Copper coupled to cast iron corroded at 2.5 mpy, which is higher than uncoupled copper.

The composition of the Petrolite corrosion probes (1018 mild steel and 99.9% copper) could not be matched precisely to that of the cylindrical specimens (A53B carbon steel and DHP copper). Since the area of the cylinders is not the same as the Petrolite probes (for which the instrument is set up to read), the corrosion rate read from the instrument must be corrected as follows:

$$\begin{array}{c}\text{true cylindrical}\\ \text{corrosion rate}\end{array} = \frac{\text{area of cylindrical specimen}}{\text{area of Petrolite probe}} \times \text{corrosion rate} \qquad (1)$$

Flow conditions are not the same at the Petrolite probes and the cylindrical specimens. Flow was controlled at 5 ft/sec at the specimen (5/8-in. ID) but was much lower at the Petrolite probes (≃2-in. ID). Examination of the data in Figure 5 shows the general corrosion behavior of a system at startup: a

TABLE 6. Results of Uniform Corrosion Tests[a]

Material	Test 1,[b] mpy	Test 3,[c] mpy
Carbon Steel		
Coupon 1	1.09	3.95
Coupon 2	1.04	3.62
Coupon 3	1.01	4.55
Mean	1.05	4.04
T316		
Coupon 1	0.01	0.02
Coupon 2	0.02	0.03
Coupon 3	0.12	0.01
Mean	0.07	0.02
T304	No Test	0.03
DHP Copper		
Coupon 1	1.12	1.84
Coupon 2	1.13	1.88
Coupon 3	0.89	2.02
Mean	1.05	1.91
Admiralty Brass		
Coupon 1	0.55	0.53
Coupon 2	0.29	0.47
Coupon 3	0.44	0.37
Mean	0.43	0.46
Titanium		
Coupon 1	0.02	+0.06 mg cm^{-2}
Coupon 2	0.04	+0.07 mg cm^{-2}
Coupon 3	0.01	No test
Mean	0.02	
Copper Coupled to Cast Iron	2.52	7.78

(a) Data provided by Radian.
(b) Conditions: T = 87°C; O_2 = 0 ppb; Reynolds number = 7.16 x 10^4; Exposure time = 808.5 h
(c) Conditions: T = 87°C; O_2 = 30 ppb; Reynolds number = 4.13 x 10^4; Exposure time = 543 h

TABLE 7. Results of Crevice Corrosion and SCC Tests[a]

Material	Test 1	Test 3
Carbon Steel	Crevice corrosion - maximum depth 1.2 mils (13 mpy). No test for SCC.	Crevice corrosion - maximum depth 3.1 mils (50 mpy). No test for SCC.
DHP Copper	Incipient crevice corrosion. No SCC detected.	Incipient crevice corrosion. No SCC detected.
Admiralty Brass	Incipient crevice corrosion. Pits 1 grain deep in area of maximum stress.	Incipient crevice corrosion. No pits in area of maximum stress.
T316	No localized corrosion. No SCC.	No localized corrosion. No SCC.
Titanium	No localized corrosion. No test for SCC.	No localized corrosion. No test for SCC.

(a) Data provided by Radian Corporation.

rapid corrosion rate that decreases within 1 to 2 days. After 2 days the steel corrosion rate is relatively constant throughout the experiment and quite insensitive to the entry of oxygen during well changes. The difference in corrosion rates during the first half of the experiment may reflect composition differences between the probes (1018 steel) and the cylindrical specimens (A53B carbon steel). Integrating the instantaneously determined corrosion rate of the steel cylindrical specimens over the duration of the experiment results in an average corrosion rate of 1.5 mpy, which compares well with the weight loss value of 1.1 mpy. The steel specimens had a thin black film that was probably a mixture of FeS, FeS_2, and Fe_3O based on a Pourbaix diagram (Biernat and Robins 1972) calculated at $100^{\circ}C$ for a pH of 7.8 and a redox potential of -0.3 V. An x-ray analysis could identify the actual film composition. The film conferred some immunity to corrosion when oxygen entered for a short period, but this may not be the case when oxygen is constantly present.

The copper system exhibited high corrosion rates at the beginning of the experiment and then rapidly decreased. However, copper responded rapidly with an increased corrosion rate (see Figure 5) when oxygen entered on the third, fifteenth, and thirty-fourth days due to changes in well operation. Integrating the instantaneously determined corrosion rates of the cylindrical specimens over the duration of the experiment results in a predicted corrosion rate of 4.6 mpy versus a weight loss value of 1.1 mpy. The Petrolite method overestimates copper corrosion rates by a factor of four and suggests that future instrument readings should be reduced by this factor. However, the increased corrosion rates due to oxygen entry are real, and it is only the magnitude of the rate that is in error. The black film on the specimens is most likely Cu_2S and CuS, but a Pourbaix diagram does not exist for conditions at 100^oC. Sulfide films are not considered to be very protective since the corrosion rate increased rapidly with the entry of oxygen. Oxygen has a greater effect on the corrosion rates of the cylindrical specimens where the flow rate is much higher, which indicates that the mass transport of oxygen may be controlling the corrosion rate.

TEST 2

Test 2 conditions were to be identical to Test 1 except that flow rates were to be a factor of 10 lower (0.5 ft/sec). The experiment began on May 21, 1979, but had to be terminated due to problems requiring repair of the OIT geothermal pump and distribution system. Flows were on and off during the summer months so that oxygen entered the experimental setup and invalidated the original test. By July the corrosion results for Test 1 were available; and the low corrosion rates indicated that Test 2 was no longer necessary, and it was aborted.

TEST 3

The experimental conditions for Test 3 included a flow rate of 5 ft/sec (4.7 gal/min), which was the same flow rate used during Test 1, and an oxygen concentration of 300 ppb. At the OIT storage tank (about 15 ft from the experiment), a pipe tee was installed and a 7-micron 316 SS filter was inserted and used as the air sparging system. The filter body was welded to a stainless tube so a pressure connection could be made. Oil-free instrument air was used as the source of oxygen. A flowmeter and pressure regulating valve controlled the flow rate. An initial flow rate of 35 cm^3/min gave an oxygen concentration at the test loop outlet of 300 ppb (measured by Chemetrics Oxygen Kit®).

Within 4 days after startup, the airflow had fallen to zero; but due to a communication failure between OIT and PNL, PNL was not made aware of this problem until the end of the experiment. At that time, the oxygen was measured at the test loop outlet to be 30 ppb. Unfortunately, it is impossible to say what the oxygen level was during the experiment. Experimental data for Test 3 are shown in Table 4, p. 14.

Radian's evaluation (Ellis 1980) of the corrosion coupons in Test 3 is reported in Tables 6 and 7, pp. 22 and 23. In summary,

- Carbon steel had a uniform corrosion rate of 4.0 mpy and a crevice corrosion rate of 50 mpy.
- Copper had a uniform corrosion rate of 1.9 mpy with some crevice corrosion but no evidence of SCC.
- Brass corroded uniformly at 0.46 mpy with incipient crevice corrosion but no evidence of SCC.
- 316 SS corroded uniformly at 0.02 mpy with no evidence of crevice corrosion or SCC.
- Titanium had a negligible uniform corrosion rate with no evidence of crevice corrosion or SCC.
- Copper coupled to cast iron showed a three-fold increase in corrosion rate over the deoxidized conditions.

Radian concluded that the low level of dissolved oxygen had a pronounced effect on the corrosion rate of carbon steel (four-fold increase) but a less dramatic effect on copper (two-fold increase).

®Chemetrics, Inc., Warrenton, Virginia.

The performance of the corrosion probes and redox electrode is shown in Figure 6. Corrosion rates for the cylindrical specimens are compensated for area using Equation (1). The integrated corrosion rate of the steel cylindrical specimens over the duration of the experiment resulted in an average corrosion rate of 9.0 mpy, which is more than two times greater than the 4.0 mpy determined by weight loss. This discrepancy may be due to the effects of crevice corrosion. The integrated corrosion rate for the Petrolite steel probes is 4.0 mpy and compares to that determined by weight loss. Since the hydrodynamic conditions are quite different at the locations of the Petrolite probes and the weight loss specimens, it appears that velocity does not have a major effect on corrosion rates. The redox potential of approximately +0.3 V (SHE) would indicate from a Pourbaix diagram (Biernat and Robins 1972) that the porous black surface film was composed of Fe_2O_3. Any iron sulfides present in the film would not be in equilibrium with the water chemistry. No x-ray analysis was carried out.

Integration of the corrosion rate of the cylindrical copper specimens resulted in an average rate of 4.0 mpy, which is two times larger than the 2.0 mpy determined by weight loss. Integration of the Petrolite copper probes resulted in an average corrosion rate of 5.9 mpy, which is an even larger estimation of corrosion rate.

Although the potential of the redox electrode slowly became more positive throughout the experiment, it is impossible to make any generalization since the oxygen content was not controlled. Assuming 30-ppb oxygen throughout the experiment, the relative response of the redox electrode was about 0.6 V when going from 0- to 30-ppb oxygen. The redox electrode is extremely sensitive to oxygen.

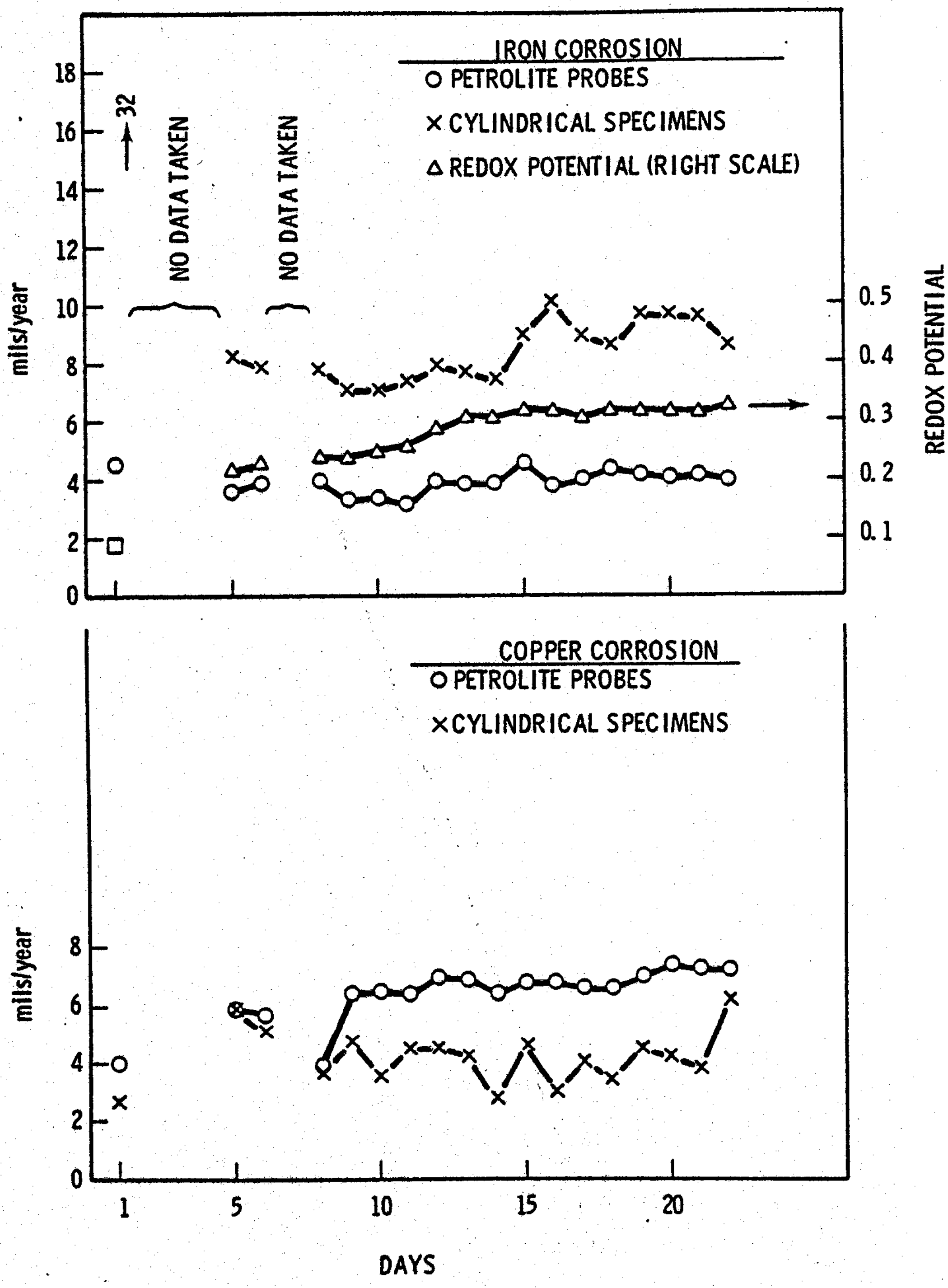

FIGURE 6. Corrosion Rates of Petrolite and PNL Probes Versus Days of Exposure, Test 3

REFERENCES

1978 Annual Book of ASTM Standards Designation G38-73. 1978. American Society for Testing and Materials, Philadelphia, Pennsylvania.

Biernat, R. J., and R. G. Robins. 1972. "High-Temperature Potential/pH Diagrams for the Iron-Water and Iron-Water-Sulphur System." Electrochemica Acta 17:1261-1283.

Danielson, M. J. 1979. "The Construction and Thermodynamic Performance of an Ag-AgCl Reference Electrode for Use in High-Temperature Aqueous Environments Containing H_2 and H_2S." Corrosion 35(2):200.

Ellis, P. F. 1980. "Coupon Evaluation Geothermal Materials Tests, Oregon Institute of Technology, Klamath Falls, Oregon." DCN 80-212-003-05, DOE Contract DE-AC02-79Et27026, Radian Corporation, Austin, Texas.

Fontana, M., and R. Staehle. 1976. Advances in Corrosion Science and Technology, Volume 6. Plenum Press, New York.

Fournier, R. O., and A. H. Truesdell. 1974. "Geochemical Indicators of Subsurface Temperature - Part 2, Estimation of Temperature and Fraction of Hot Water Mixed with Cold Water." J. Research U.S. Geol. Survey 2(3):263-270.

Watson, J. C. July 1978. Sampling and Analysis Methods for Geothermal Fluids and Gases. PNL-MA-572, Pacific Northwest Laboratory, Richland, Washington.

DISTRIBUTION

No. of
Copies

OFFSITE

A. A. Churm
DOE Patent Division
9800 S. Cass Avenue
Argonne, IL 60439

2 A. J. Adduci
Division of Geothermal Energy
U.S. Department of Energy
San Francisco Operations Office
1333 Broadway
Oakland, CA 94612

S. M. Hansen
Systems and Procedures Section
DOE Energy Technology Systems
Mail Station 404,
600 E. Str., NW
Washington, DC 20545

2 R. R. Reeber
Mail Stop 3344 RA 233
Division of Geothermal Energy
U.S. Department of Energy
1200 Pennsylvania Avenue, NW
Washington, DC 20461

27 DOE Technical Information Center

J. W. Arlidge
Nevada Power Company
P.O. Box 230
Las Vegas, NV 89151

E. Backstrom
U.S. Department of the Interior
Bureau of Reclamation
Engineering and Research
Center
P.O. Box 25007
Bldg. 67, Federal Center
Denver, CO 80225

No. of
Copies

J. Barkman
Republic Geothermal, Inc.
11823 E. Slauson Avenue, Suite 1
Santa Fe Springs, CA 90670

I. Barnes
U.S. Geological Survey
345 Middlefield Road
Menlo Park, CA 94025

H. K. Bishop
San Diego Gas & Electric Co.
P.O. Box 1831
San Diego, CA 92112

R. W. Bowman
Oilwell Research, Inc.
2419 E. Main Street, Suite E
Ventura, CA 93003

A. J. Chasteen
Union Oil Co. of California
135 Main Street
Brawley, CA 92227

D. Christopherson
Union Oil Co. of California
P.O. Box 76
Brea, CA 92621

M. Conover
Radian Corporation
8500 Shoal Creek Road
Austin, TX 78766

G. W. Crosby
Phillips Petroleum Company
11526 Sorrento Valley Road
San Diego, CA 92121

G. Culver
Geo-heat Utilization Center
Oregon Institute of Technology
Klamath Falls, OR 97601

No. of
Copies

F. J. Dodd
Pacific Gas & Electric Co.
3400 Crow Canyon Road
San Ramon, CA 94583

P. Ellis
Radian Corporation
8500 Shoal Creek Road
Austin, TX 78766

J. Farison
Union Oil-Geothermal
P.O. Box 6854
Santa Rosa, CA 95401

J. Featherstone
2120 South 9th Street
El Centro, CA 92243

R. O. Fournier
U.S. Department of Interior
Office of Geochemistry and
Geophysics
345 Middlefield Road
Menlo Park, CA 94025

C. Grigsby
CNC-2 M.S. 738
Las Alamos Scientific Laboratory
Las Alamos, NM 87545

R. L. Hall
Geothermal UPD
EG&G Idaho, Inc.
P.O. Box 1625
Idaho Falls, ID 83401

J. H. Hill
Lawrence Livermore Laboratory
P.O. Box 808, L-325
Livermore, CA 94550

T. C. Hinrichs
Imperial Magma
P.O. Box 2082
Escondido, CA 92025

No. of
Copies

J. Kuwada
Rogers Engineering
16 Beale Street
San Francisco, CA 94105

P. N. LaMori
Occidental Research Corporation
2100 S. E. Main Street
P.O. Box 19601
Irvine, CA 92713

W. C. Lieffers
Union Oil Co. of California
Research Department
P.O. Box 76
Brea, CA 92621

2 P. Lineau
Oregon Institute of Technology
Klamath Falls, OR 97601

F. X. McCawley
U.S. Department of the Interior
Bureau of Mines
College Park, MD 20740

R. McCurdy
PG&E, Dept. of Engineering
Research
3400 Crow Canyon Road
San Ramon, CA 94583

R. L. Miller
EG&G Idaho, Inc.
307 Second Street
Idaho Falls, ID 83401

R. E. Moran
U.S. Geological Survey, WRD
M.S. 415, Federal Center
Denver, CO 80215

L.P.J. Muffler
U.S. Geological Survey
345 Middlefield Road
Menlo Park, CA 94025

No. of
Copies

C. L. Nealy
Atomics International
8900 DeSoto Avenue
Canoga Park, CA 91304

C. Otte
Union Oil Co. of California
P.O. Box 7600
Los Angeles, CA 90017

R. Potter
Occidental-Research Corporation
P.O. Box 19601
Irvine, CA 92713

M. G. Reed
Chevron Oil Field Research Co.
P.O. Box 446
La Habra, CA 90631

R. A. Reynolds
GHT Laboratories
106 South 8th Street
Brawley, CA 92227

W. D. Riley
U.S. Bureau of Mines
College Park Metallurgy
Research Center
College Park, MD 20740

V. Roberts
Electric Power Research
Institute
P.O. Box 10412
Palo Alto, CA 94304

F. Schoepflin
Bechtel Corporation
50 Beale Street
San Francisco, CA 94105

F. W. Schremp
Chevron Oil Field Research Co.
P.O. Box 446
La Habra, CA 90631

No. of
Copies

M. C. Smith
Los Alamos Scientific Laboratory
P.O. Box 1663
Los Alamos, NM 87544

R. C. Sones
Westec Services, Inc.
East Mesa Test Site
P.O. Box 791
Holtville, CA 92250

T. Springer
Rockwell International
Atomics International Division
8900 DeSoto Avenue
Canoga Park, CA 91304

W. J. Subcasky
Chevron Oil Field Research Co.
P.O. Box 446
La Habra, CA 90631

D. Suciv
EG&G Idaho Inc.
307 Second Street
Idaho Falls, ID 83401

J. M. Thompson
U.S. Geological Survey,
Geologic Division
Branch of Exp. Geochemistry
and Mineralogy
345 Middlefield Road
Menlo Park, CA 94025

University of Hawaii at Monoa
2424 Maili Way
Honolulu, HI 96822

T. Veneruso
Sandia Laboratory
Albuquerque, NM 87185

O. Vetter
Vetter Associates
3189 C Airway Avenue
Costa Mesa, CA 92626

No. of
Copies

R. N. Wheatley
Union Oil Co. - Research Center
P.O. Box 76
Brea, CA 92621

ONSITE

DOE Richland Operations Office

H. E. Ransom

50 Pacific Northwest Laboratory

J. Britton
M. J. Danielson (25)
R. L. Dillon (2)
J. R. Divine
J. L. Duce
S. K. Edler
D. H. Getchell
B. Griggs
C. R. Hann
G. A. Jensen
D. Jones
C. H. Kindle
O. H. Koski
P. Morrow
L. D. Perrigo
D. W. Shannon
R. P. Smith
R. G. Sullivan
Publishing Coordination Fe(2)
Technical Information (5)